Ecological Informatics 5 (2010) 390–399

Contents lists available at ScienceDirect

Ecological Informatics

journal homepage: www.elsevier.com/locate/ecolinf

Developing a photosynthetic sterility model to estimate CO_2 fixation through the crop yield in Asia with the aid of MODIS data

Daijiro Kaneko [a,*], Peng Yang [b], P.J.-F. Yeh [c], Toshiro Kumakura [d]

[a] Remote Sensing Environmental Monitor, Inc., 4-5-5, Kamariya-nishi, Kanazawaku, Yokohama, Kanagawa, 236-0046, Japan
[b] Key Laboratory of Resources Remote Sensing & Digital Agriculture (Ministry of Agriculture); Institute of Agricultural Resources & Regional Planning, Chinese Academy of Agricultural Sciences, 12, Zhongguancun South Street, Haidian District, Beijing, 100081, PR China
[c] Institute of Industrial Science, 4-6-1 Komaba, Meguro-ku, Tokyo, University of Tokyo, 153-8505, Japan
[d] Department of Civil and Environmental Engineering, Nagaoka University of Technology, 1603-1, Kamitomioka, Nagaoka, Niigata, 940-2188, Japan

ARTICLE INFO

Article history:
Received 1 February 2010
Received in revised form 12 July 2010
Accepted 16 July 2010

Keywords:
Photosynthesis rate
Yield
Monitoring
Modeling
Validation
CO_2
Carbon
Fixation
Rice
Crop
Remote sensing
Partitioning
Land-cover classification
MODIS
SPOT
GMS

ABSTRACT

Remote sensing technologies have been advanced continuously to a certain level for multi-scale applications to ease social and political concerns resulting from food security. In this study, an integrated monitoring, sensing and modeling system for estimating CO_2 fixation and grain yields using a photosynthetic sterility model was developed. Input data for model computation include observed meteorological data, numerical prediction reanalysis data, and satellite data such as solar radiation, land-cover and Normalized Difference Vegetation Index (NDVI) on a continental scale. Model validation requires crop yields and the Crop Situation Index (CSI) was provided by the Japanese government. It also demonstrates the application potential of this system to grain fields of paddy rice, winter wheat, and maize in Southeast Asia. The carbon hydrate in grains has the same chemical formula as that of cellulose in grain vegetation. The partition of sequestered CO_2 into grain, straw, and root portions of plant biomass weight was computed. The present photosynthesis model was evaluated using the mass of carbon included in the harvested grains of provincial crop production. Results indicate that the proposed system successfully estimates the photosynthesis fixation of rice reasonably well in Japan and China through the analysis of carbon in grains. However, the model tends to underestimate the photosynthesis rates for winter wheat and maize. The parameterization of radiation response function and the temperature response functions for low-temperature sterility need to be improved in the future.

1. Introduction

The sustainable crop production in the world has become uncertain in terms of food security under climate change, economic development, and population growth and migration. The food crisis might be worse in the future due to insufficient crop production in developed countries and growing demand for food driven by economic development in developing countries. Remote sensing technologies have been advanced continuously to a certain level for multi-scale applications to ease social and political concerns resulting from food security. The network of Global Earth Observation System of Systems (GEOSS) assesses agricultural production as its main area of social benefit (see the reference, GEO GEOSS, 2009). Many studies have expanded the scale of monitoring crop production from farm field for precision agriculture to province and state levels. However, national, continental, and global scale crop monitoring systems remain difficult to develop due to the lack of quality data for the modeling.

In this study, an integrated monitoring, sensing and modeling system for estimating CO_2 fixation and grain yields using a photosynthetic sterility model was developed. This system integrates the effects of solar radiation and air temperature on photosynthesis along with grain filling from heading to ripening. Monitoring crop production using remotely sensed data and daily meteorological data can provide important early warning for poor crop production. Grain production monitoring is expected to support crisis management and thereby maintain food security in Asia, which faces climate fluctuation that is expected to persist during this century of global warming (IPCC, 2009; ERIA, 2008). Prices of grains have tripled over the last decade, and show instability caused by global financial uncertainty (see the reference, Food Outlook, 2009). The mechanism-based

* Corresponding author.
E-mail addresses: kand.rsem@gmail.com (D. Kaneko), yangpeng@mail.caas.net.cn (P. Yang), patyeh@rainbow.iis.u-tokyo.ac.jp (P.J.-F. Yeh), kumakura@vos.nagaokaut.ac.jp (T. Kumakura).

1574-9541/$ – see front matter
doi:10.1016/j.ecoinf.2010.07.008

indices such as the Crop Production Index (CPI) and Unit CPI (CPI_U) are defined in this paper by using a satellite-based photosynthesis model to monitor crop yields on a continental scale. The proposed index, CPI_U, sets the amount of growth as known by using the Normalized Difference Vegetation Index (NDVI) data. Such an index also incorporates estimates of the instantaneous photosynthesis rate (PSN) as well as low-temperature sterility and high-temperature injury from the heading to the ripening stages.

Crop fields are classified using a decision-tree method with MODIS land-cover data, the NDVI, and Land Surface Water Index (LSWI) indices derived from Système Pour l'Observation de la Terre (SPOT) VEGETATION data. The fundamental land-cover data are supplied by the National Aeronautics and Space Administration (NASA) Goddard Space Flight Center (GSFC) (2010). The LSWI was used by Xiao et al. (2005) for paddy classification with the index NDVI. This study also provides spatial distributions of the photosynthesis (PSN) and Net Primary Production (NPP) pixel wise measures, which reflect the CO_2 fixation in Asian areas, based on the land-cover classification described above. One validation method is to compare the carbon weight included in harvested grains with photosynthetically fixed grain carbon, which is computed using our model, by partitioning sequestered CO_2 into rice starch, and cellulose included in straw and root portions of plant biomass. Carbon partitioning itself is studied by crop scientists (Sasaki et al., 2005; Yoneyama et al., 1989), but it has never been reported as used for validation in so many crop models. We propose this validation method using the partitioning of carbon to verify the accuracy of grain plant photosynthesis models.

Numerous studies on grain production monitoring at the farm and province scale are available in literature (e.g., Hayes and Decker, 1996; Idso et al., 1977; Tubiello et al., 2002). However, most of these studies were conducted in the U.S. where they export most grains in the world (FAO FAOSTAT, 2007), and most of them focused on wheat and corn rather than rice. Studies of national-scale crop production monitoring in China or India were reported by Gao et al. (1998) and Kogan et al. (2005). Moreover, remote sensing data were extensively used in previous crop yield prediction studies (e.g., Gonzalez et al., 2002; Roebeling et al., 2004; Wiegand et al., 1986). However, most of the models in these studies (Cavero et al., 2000; Doraiswamy et al., 2004; Jones et al., 2003) are complex and contain numerous empirical constants as well as vertical distributions of soil moisture. Doraiswamy et al. (2005) combined the data from the Scattering by the Arbitrarily Inclined Leaves (SAIL) model and Moderate Resolution Imaging Spectroradiometer (MODIS) by estimating the maize Leaf Area Index (LAI) in rural Illinois. Dente et al. (2008) assimilated LAI data into the crop growth model CERES (Crop Environment Resource Synthesis) to improve the accuracy of wheat yield predictions at the regional scale, with their LAI maps retrieved from the ENVISAT Advanced Synthetic Aperture Radar (ASAR) and the Medium Resolution Imaging Spectrometer (MERIS) data. Fang et al. (2008) presented data assimilation approaches to combine the CERES model and LAI from MODIS in the corn yield estimation. However, the scale of application is only 110 km^2 in Dente et al. (2008) and not horizontal but only separated point sites in the Indiana State in Fang et al. (2008). The CERES models for principal grains have the concept of daily dry matter production based on the heat unit defined by air temperatures. The combination of models and remotely sensed data are useful approaches for farm-scale management by precision agriculture. In this study, we assimilated the data of NDVI from SPOT VEGETATION, solar radiation from the Japanese Geostationary Meteorological Satellite (GMS) Center, air temperature from global weather data, MODIS land-cover data, and ground observed meteorological data to develop a photosynthetic sterility model (Kaneko et al., 2009b). Also, solar radiation data are assimilated by using reanalysis data from the National Centers for Environmental Prediction (NCEP) and the European Center for Medium-range Weather Forecasts (ECMWF) in addition to the GMS data.

The crop production indices such as CPI and CPI_U defined in the next section to monitor grain production have been developed as the photosynthesis-sterility Crop Production Index, incorporating the effects of temperature on the photosynthesis rate and on the sterility during grain filling from heading to ripening, in our previous studies (Kaneko, 2006a,b,c, 2007; Kaneko et al., 2003, 2004a,b, 2005, 2008a,b, 2009a,b). The CPI_U index depends on solar radiation, temperature and vegetation biomass (represented as NDVI from SPOT VEGETATION). In view of climate change and the associated variations in annual rainfalls in Asian countries, it is important to monitor the quantity of grain production at an early stage. Continuous monitoring of crop production using the predictive indices CPI and CPI_U can support the management of food security over Southeast Asia, particularly in world major grain importers like China and Japan.

Asian governments are advancing negotiations to accommodate and maintain rice reserves to reduce the threat of food crises resulting from poor production in Asian countries, in addition to the East Asia Emergency Rice Reserve (EAERR) and other worldwide services such as the Foreign Agricultural Service (FAS) of the United States Department of Agriculture (USDA), Monitoring Agricultural ResourceS (MARS) of the European Commission, and the Global Information and Early Warning System (GIEWS) of Food and Agriculture Organization (FAO) of the United Nations. Nevertheless, the present scale of that storage is less than 1/10 of the necessary reserves because grain storage requires huge budget outlays annually. Furthermore, conventional monitoring services do not produce computed results but a result obtained using synthesized meteorological information with vegetation indices derived from satellites. Crisis management by crop monitoring using this numerical yield model with the GEOSS network can help many countries, especially nations that are not self-sufficient in grain production, to avert or mitigate looming social, economic, and political tensions.

2. Model development and validation

2.1. Model for monitoring crop production

The model developed in this study elucidates the effects of low-temperature sterility and high-temperature injury on crop yields in addition to accounting for the mechanism of photosynthesis. These concepts are necessary for monitoring rice production on a continental scale. Sterility of plants in tropical areas, caused by low temperatures in paddies, affects yields during the plant flowering stage by causing sterility on pollination in the temperate zone. The photosynthesis rate (PSN) is defined below in Eq. (1a) with a Michaelis–Menten type of radiation response function f_{rad_mm}, which is proper for wheat and maize, and another type of radiation response function f_{rad_pc} proposed by Prioul and Chartier (1977), which properly fits the curve of the photosynthesis rate for paddy rice:

$$PSN = f^{\bullet}_{rad}\, f_{Syn}(T^{\bullet}_c)\beta^{\bullet}_s\, eLAI \tag{1a}$$

$$f_{rad\_mm} = \frac{a_{mm}\cdot PAR}{b_{mm} + PAR} \tag{1b}$$

$$f_{rad\_pc} = \frac{a_{pc}\cdot PAR + PSN_{\max} - \sqrt{\left(a_{pc}\cdot PAR + PSN_{\max}\right)^2 - 4c_c\cdot a_{pc}\cdot PSN_{\max}PAR}}{2c_c} \tag{1c}$$

where f_{rad} equals to f_{rad_mm} in Eq. (1b) for wheat and maize, and equals to f_{rad_pc} in Eq. (1c) for rice. Also, PSN is the photosynthesis rate ($gCO_2/m^2/day$), PAR denotes the photosynthetically active radiation (MJ/m^2), β_s is the stomatal opening (no dimension), a_{mm} ($gCO_2/MJ/day$) and b_{mm} (m^2/MJ) are Michaelis–Menten constants, T_c represents the canopy temperature (°C), eLAI stands for the effective leaf area index (no dimension), a_{pc} is the Prioul–Chartier constant (dimensionless), PSN_{max} is the maximum PSN (gCO_2/m^2/day), and c_c is the curve convexity constant (dimensionless).

The effect of chlorophyll on PSN is expressed using NDVI (which approximates the variable used for eLAI; Kaneko, 2006a,b,c). In similar studies conducted earlier, Aase and Siddoway (1981) directly related NDVI to the spring wheat yield. Rasmussen (1992, 1998) advanced assessment of time integrals of NDVI to PSN and Net Primary Production (NPP). The unit of the photosynthesis rate in this model is the carbon dioxide fixation rate (gCO_2/m^2/day), which fits the objectives for carbon circulation on earth in the era of climate change. The stomata β_s is expressed using the Crop Water Stress Index (CWSI), which is defined as the ratio of actual evapotranspiration (E_{ac}) divided by the Penman potential evaporation (E_p). However, β_s does not affect the PSN in the case of paddy areas because of irrigation, which creates semi-submerged plants in shallow water. The values of E_{ac} and E_p are supplied from ECMWF to compute horizontal distributions of the PSN. We also applied a complementary model to monitor paddy yields at Japanese sites and at Nanjing, China, using meteorological data for the accuracy evaluation of E_{ac} and E_p supplied from ECMWF.

Even if leaf areas index is larger than 1, the energy available for use in crop photosynthesis never exceeds the amount of the sunlight energy falling at a right angle on a single area of the earth surface. The solar energy concept of photosynthesis indicates that the maximum eLAI is equal to 1. The eLAI is approximated by NDVI, which includes the effects of chlorophyll amounts and effective leaf areas for photosynthesis. Furthermore, NDVI is theoretically less than 1. The concept of the effective leaf area is clear from the energy budget perspective to model the photosynthesis rate. On the other hand, LAI is valuable for evaluating the vegetation biomass. We consider that inclined leaves of crop plants scatter and reflect incoming light from one another. The eLAI in the case of crop plants with dense leaves could therefore be slightly larger than 1.

The temperature response function of the photosynthesis rate f_{Syn} is such that the rate PSN falls at low air temperatures. The function f_{Syn} shows an S-shaped curve defined by Eq. (2), which is well known as the sigmoidal logistic type function:

$$f_{Syn}(T_c) = \left[\frac{1}{1+\exp\left\{k_{syn}(T_c - T_{hv})\right\}}\right], \tag{2}$$

where T_{hv} is the temperature parameter at half of the maximum photosynthesis rate (°C), and k_{syn} is the gradient constant of the relation between the function $f_{Syn}(T_c)$ and the canopy temperature, which is approximated by the air temperature at 2 m above the ground surface.

The temperature response functions for the low-temperature sterility and high-temperature injury can be defined as the following equations (Vong and Murata, 1997):

$$f_{Lster}(T_c) = 1 - \exp\left[k_{Lster}(T_{Lster} - T_c)\right] \tag{3a}$$

$$f_{Hster}(T_c) = 1 - \exp\left[k_{Hster}(T_c - T_{Hster})\right], \tag{3b}$$

In those equations, k_{Lster} is the low-temperature sterility constant, T_{Lster} is the low-sterility limit temperature (°C), k_{Hster} is the high-temperature injury constant, T_{Hster} is the high-injury limit temperature (°C), and T_c is the plant leaf temperature (°C).

Finally, the response function of the compounded temperature sterility affects both low-temperature and high-temperature injuries in grain production, as expressed in the following equation:

$$F_{Ster}(T_s) = f_{Lster}(Tc) \cdot f_{Hster}(T_c) \tag{4}$$

It is necessary to normalize the effective LAI (represented by NDVI), which differs among monitoring sites because the vegetation cover ratio includes other land-cover, soils, and breeds of crop plants. Computed values of CPI under almost identical meteorological conditions may differ because NDVI varies among different regions in Japan, even if the yields are equal. Despite having an equivalent harvest yield, the large NDVI certainly causes overestimation of PSN and yields in the province. To elucidate the effects of growth and other factors on the CPI, a standardized NDVI, called the Unit NDVI, is defined in this study as dividing the NDVI by its value corresponding to average yield over the current season as follows:

$$NDVI_{U,i} = \frac{NDVI_i}{NDVI_{H100}}, \tag{5}$$

where $NDVI_{U,i}$ stands for the Unit $NDVI$ on the i-th day, $NDVI_i$ denotes the NDVI on the i-th day, and $NDVI_{H100}$ signifies the NDVI on the ripening day, based on the average annual yield.

The following normalized photosynthesis rate is used for CPI_U.

$$PSN_U = \frac{PSN}{iPSN_{100}}, \tag{6}$$

where the PSN_U represents the normalized photosynthesis rate; $iPSN$ (gCO_2/m^2) is the integrated photosynthesis rate from sowing to the end of the harvesting stage, and $iPSN_{H100}$ is defined by the averaged iPSN as a photosynthetic indicator of the normal crop production at the harvesting stage in a region, that is, the crop situation index (CSI) is equal to 100. The CSI is the ratio of crop production in a certain year to the mean production over ten most recent years obtained at harvest. The objective of the normalization in Eq. (6) is to remove regional factors due to different characteristics in each province.

The Crop Production Index (CPI, gCO_2/m^2) at harvest is defined in Eq. (7) as follows:

$$CPI = F_{Ster}(T_c) \cdot \int_{t_s}^{t_h} PSN \cdot dt \tag{7}$$

The CPI index at harvest is formed as a mechanism-based type of grain production index. The integration of photosynthesis rate in Eq. (7) over the interval from sowing t_s to harvest t_h must be multiplied by the temperature sterility function F_{Ster}. The normalization of CPI defines the dimensionless unit Crop Production Index (CPI_U) by using the normalized PSN_U as expressed in Eq. (6):

$$CPI_U = F_{Ster}(T_c) \cdot \int_{t_s}^{t_h} PSN_U \cdot dt \tag{8a}$$

$$F_{Ster} = \int_{t_f}^{tr} f_{Ster}(T_c) \cdot dt, \tag{8b}$$

where t_f is the start time of flowering (day), and t_r is the time of ripening (day).

The objective of the normalization is to make the PSN dimensionless, thereby removing noisy factors which originate from characteristics in that province.

The CPI_U defined in Eq. (8a) involves the heading term expressed via Eq. (8b), which accounts for the effect of temperature on flowering, pollination and ripening. The CPI_U at plant stages is expressed in reference to the study by Tanno et al. (2001) as follows: During crop plant stage 1 of growth, crop production depends solely on the integration of PSN_U. It is defined as the integration of PSN from t_s to t as follows:

$$CPI_U = \int_{t_s}^{t} PSN_U \cdot dt \tag{9}$$

and during the crop plant stage 2, which includes booting, heading, and flowering to ripening:

$$CPI_U = F_{Ster}(T_c) \cdot \int_{t_s}^{t} PSN_U \cdot dt \tag{10a}$$

$$F_{Ster} = \int_{t_f}^{t} f_{Ster}(T_c) \cdot dt \tag{10b}$$

and during the crop plant stage 3 of harvesting:

$$CPI_U = F_{Ster}(T_c) \cdot \int_{t_s}^{t_r} PSN_U \cdot dt \tag{11a}$$

$$F_{Ster} = \int_{t_f}^{tr} f_{Ster}(T_c) \cdot dt \tag{11b}$$

where t_f is the start time of flowering and t_r is the time of ripening.

The time intervals of F_{Ster} in the CPI_U differ from those of other plant stages because sterility affects yields for only a limited duration of flowering and pollination.

2.2. Method for model validation

The validation is based on pursuing the weight of carbon that is fixed in grains by photosynthesis using the developed model, in which the unit of the photosynthesis rate is expressed not in terms of biomass or energy but in terms of CO_2 sequestration. Crop yields can also provide the weight of carbon in grain according to the chemical formula of starch as $(C_6H_{10}O_5)_n$. Some crop scientists (Kato et al., 2006; Sasaki et al., 2005; Yoneyama et al., 1989) have investigated carbon partitioning in rice to elucidate carbon, nitrogen, and root effects on rice photosynthesis and production. Validation of the photosynthetic sterility model uses carbon weights included in provincial harvested grain yields by comparison with the values computed using the present model. Fig. 1 depicts the partitioning of sequestered CO_2 into rice, straw, and root portions of plant biomass from related references of carbon partitioning by Yoneyama et al. (1989) and the Harvest Index by Sinclair (1998) and Cui et al. (2000). The percentage of the carbon included in grain weight and sterility effects calculated from CSI values is useful to evaluate the model performance of yield estimation by determining the weight of carbon sequestered in plant grains.

This paper presents the first effort to use carbon partitioning data to validate a crop production model using the chemical formulae of cellulose and starch sequestered by plant photosynthesis.

3. Data

The photosynthesis (CO_2 fixation) rate PSN requires daily solar radiation and air temperature data not only for computing the CPI_U index for grain production monitoring, but also for evaluating carbon cycle and biomass energy processes. The operational aim of monitoring the quantity of crop production in Southeast Asia demands daily data for solar radiation and air temperatures across large regions. A useful source of the meteorological data is the world weather data network, which currently gives daily weather reports of data around the world in real time. However, these are point data at meteorological observation sites. Therefore, in this study the atmospheric reanalysis data supplied by ECMWF in EU and NCEP in the USA will be used, which include the gridded surface meteorological data on a global scale. In addition, the ground air temperature data at 10 sites in the test provinces are supplied by the Japanese Meteorological Agency from the Automated Meteorological Data Acquisition System (AMeDAS).

The Japanese Ministry of Agriculture, Forestry and Fisheries (MAFF) provides statistical information of rice yields, which includes the CSI value for paddy rice at 10 provinces. Crop seeding and harvest calendars are provided by the statistical information offices of the district agricultural administrative bureaus of MAFF upon our request. Fig. 2 portrays the distribution of vegetation index NDVI derived from SPOT VEGETATION in eastern Asia, and the modeling sites for validation. The NDVI is used as an index of vegetation biomass for crop production indices of CPI and CPI_U. The irradiance data are supplied by Japanese meteorological observatories, Japanese GMS, and the ECMWF. The satellite irradiance data are used for computing the CPI and CPI_U over Asian countries other than Japan. In addition, calendars of crop seeding and harvesting for winter wheat and maize are provided by the Food and Agriculture Organization (FAO) and the United States Department of Agriculture (USDA) for Asian countries.

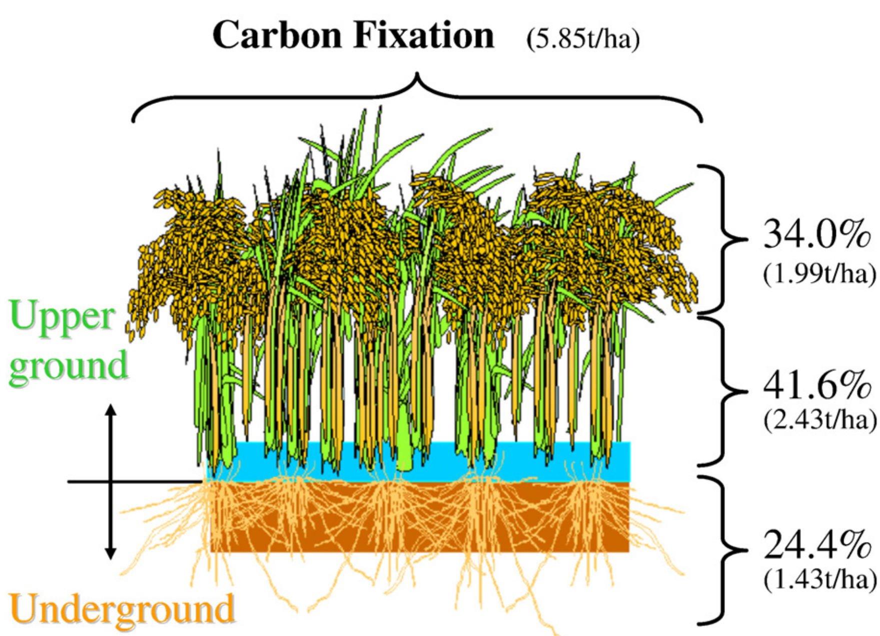

Fig. 1. Carbon partitioning in paddy vegetation, as depicted using reported data.

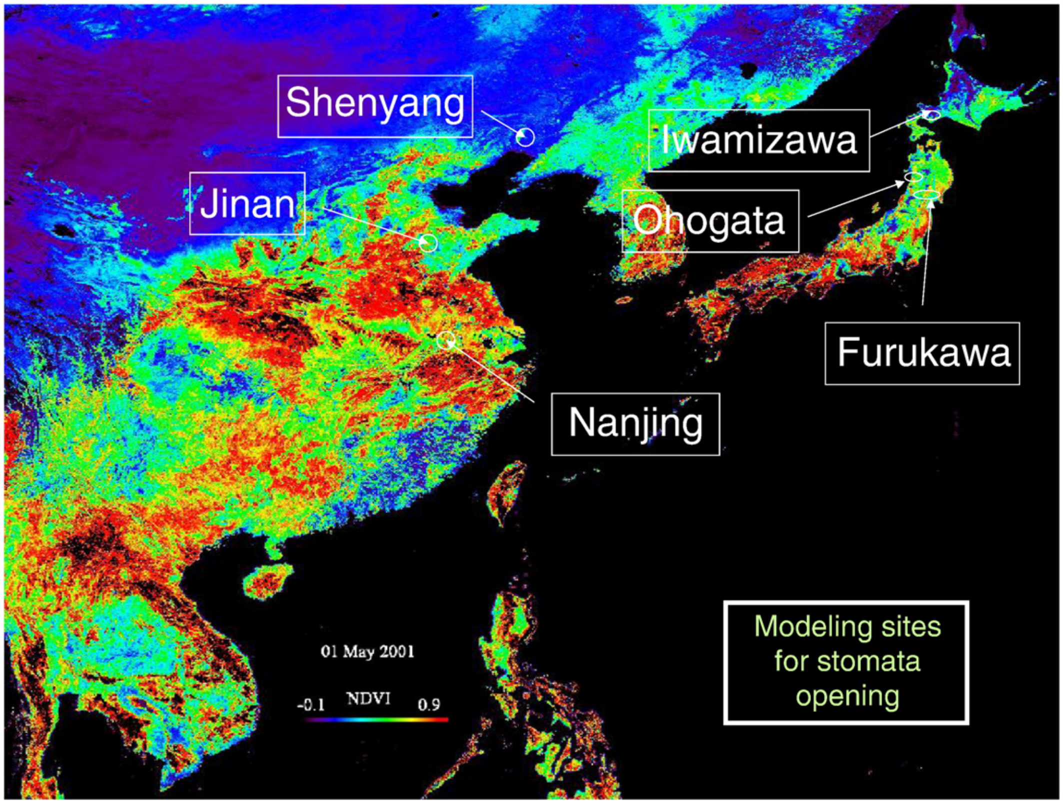

Fig. 2. Modeling sites in eastern Asia, including Japan, used for validation with the base of NDVI derived from SPOT VEGETATION.

The satellite NDVI data used in the CPI_U index are those of a 1 km mesh set of vegetation index data derived from SPOT VEGETATION. The classified 4 croplands have the same grid size of 1 km. The NDVI data derived from NOAA Advanced Very High resolution Radiometer (AVHRR) by Tateishi (2001) during 1993–1999 are used for computation of CPI and CPI_U at validation sites of paddy areas in Japan. The values of the vegetation index at the AMeDAS sites are extracted by calculating the position using the relation between latitude-and-longitude and the number of pixels of the dataset. Summarizing the input data for the computation of this model, those are meteorological data such as air temperature, solar radiation, and satellite data on NDVI used to compute PSN and CPI_U. Validation requires crop statistical data, i.e. yields and CSI on the ground. The CSI is sufficiently accurate for validation. The values of CSI are counted systematically in all provinces by MAFF as part of the administrative activities by the Japanese government. The base grid size to compute PSN is 1 km resolution, which is the pixel size of the SPOT VEGETATION. Meteorological data related to air temperature and solar radiation are available for a 0.5 degree grid, as extrapolated from meteorological reanalysis data. The PSN is computed horizontally in a 1 km grid with a 10-day interval. On the other hand, daily meteorological data observed by AMeDAS are used in special monitoring sites for the model validations for the respective computations of PSN and CPI_U.

4. Results

The CPI_U index has incorporated the main factors related to grain production. It is applicable to significant climate changes and abnormal weather conditions because of its basis in photosynthesis and sterility. Fig. 3 presents seasonal changes of the PSN during the worst production year (1993) and the best production year (1994) at the Furukawa site in the Miyagi prefecture of northern Japan. The PSN in 1993 is in general lower due to the relative lack of solar radiation and low air temperature in that year, while the PSN in 1994 is in general higher because of sufficient radiation and high air temperature. The effects of the two types of radiation response functions on PSN are compared in Fig. 3. The applicability of the functions depends on grains, grassland and forest. Fig. 4 plots the relation between the CSI index and the values of computed CPI_U at 10 monitoring sites, with the three main mechanisms of photosynthesis, low-temperature sterility, and high-temperature injury indicated. As clearly shown in Fig. 4, the low-temperature sterility causes severely poor harvests whose CSI drops sharply with the decrease of CPI_U. The photosynthesis rate for the CPI_U less than 1 (Fig. 4) decreases concomitantly with the diminution of the CPI_U because of insufficient solar radiation or lower daily accumulation of air temperature. The ability of CPI_U to discriminate three yield mechanisms is demonstrated in Fig. 4. Fig. 5(a) and (b) respectively shows the interannual variability of

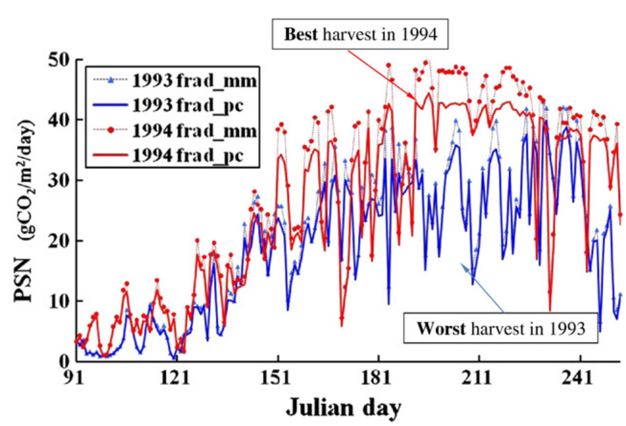

Fig. 3. Seasonal variations of the computed photosynthesis rate, including worst and best harvest cases at the Furukawa site in northern Japan.

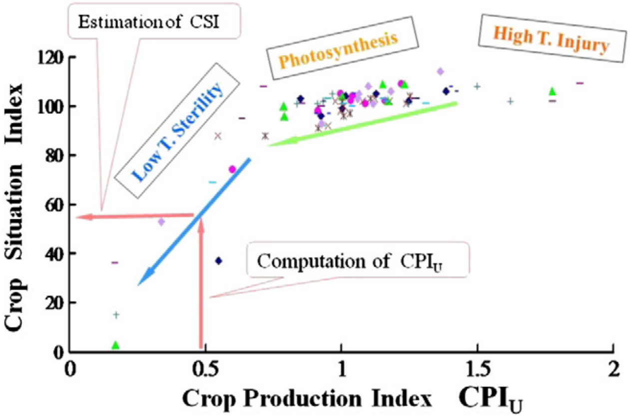

Fig. 4. Relation between computed CPI_U and CSI showing the three mechanisms of photosynthesis, low-temperature sterility, and high-temperature injury.

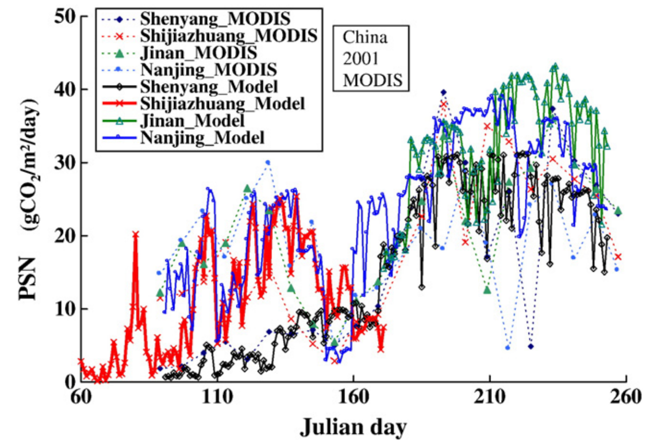

Fig. 6. Comparison of PSN computed using the present model and the MODIS PSN.

estimated CPI_U index for early monitoring of rice production at the Furukawa site in Japan and Nanjing site in China. The normalized cumulative CPI_U is the highest in the good meteorological conditions of 2005, whereas the 2003 with the second worst meteorological condition in the recent 20 years, has the lowest CPI_U (Fig. 5a). For the Nanjing site in China, CPI_U curves in Fig. 5(b) show similar values with no sterility effects of cold weather because of the relatively hot climate in southern China. The CPI_U index shows a skillful ability for crop production monitoring and early warning of poor harvests. Comparisons of the solid lines of the model's values and the dotted lines of MODIS seasonal PSNs show similar trends, as demonstrated in Fig. 6. However, MODIS PSN shows the daily net photosynthesis in contrast to the present PSN in the daytime. Solid lines of the present model tend to rise on the upper side of the dotted lines of MODIS PSN. Validation of this model using carbon partitioning method must reduce the night respiration from the photosynthesis rate that is computed using this model.

The crop fields of MODIS fundamental land-use distribution are classified into four cultivation modes—rice, winter wheat, spring wheat, and other crops—using an expert type of decision-tree method with two factors: vegetation phenology and water surface detection of the LSWI (Xiao et al., 2006; Xiao et al., 2005). Paddy fields can be discriminated by water surfaces and seasonal variation of NDVI, which drops suddenly after harvesting. Winter wheat has NDVI variation: it falls in late spring. Maize is the major crop in northeastern China. However, the corn fields are usually mixed with fields of spring wheat and soybean in the same areas. The NDVI phenology of seasonal variation of maize in the MODIS crop land settled the areas of maize in the Northeast China Plain. Cropland pixels different from these conditions are classified in the class of other crops. Fig. 7 shows a distribution of photosynthesis rate (CO_2 fixation) in grain fields during most severe drought conditions in the Northeast China Plain. The red color in winter wheat areas in the Hebei Plain exhibits a high photosynthesis rate in May in central China, compared with PSN at the corn areas in Northeast China Plain. The winter wheat is the heading to the filling stages in the Hebei Plain. In contrast, the reason of small PSN in the corn areas is that the air temperature is still low in May in the Northeast China Plain.

Table 1 presents validation cases of the photosynthesis model by partitioning carbon weights included in plant biomass of cellulose $(C_6H_{10}O_5)_n$ in aboveground leaves and stems, extracting carbon contained as starch in grains expressed using the same chemical formula. The validation table presents carbon weights in the crops of rice, winter wheat, and maize. The calculation processes of model validation on the side of data for crops harvested in provincial crop fields include calculation of dry weights of three crop types: the ratio of carbon included in CO_2, carbon contained in harvested yields, carbon included in the grain portion of crop plants per unit area, and the provincial amount of carbon fixation. On the other hand, the estimated CO_2 computed using the photosynthesis model in Table 2 gives the carbon weight included in grains by the following process. The first is calculation of net fixation by reducing nighttime respiration. The daytime respiration is already included in daily photosynthesis. The next step is the unit conversion from (gCO_2/m^2) to the harvesting statistical unit of (tC/ha). Thirdly, carbon fixation aboveground is necessary for extracting the grain portion of plant biomass. Fourth, the carbon partitioning method is useful to calculate carbon weight that is sequestered only in the grain portion using the Harvest Index, which is defined by the weight of grain and aboveground plants. The last is a

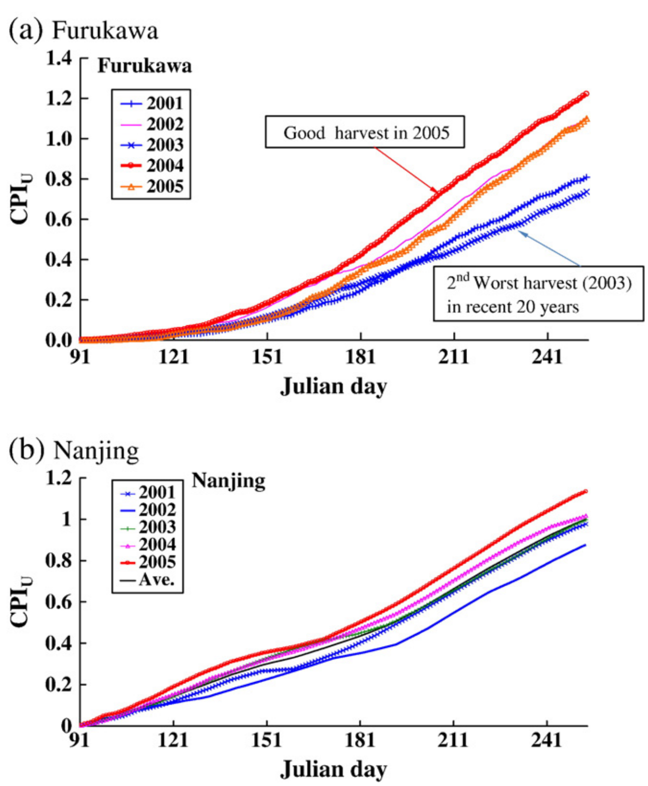

Fig. 5. Seasonal variations of the crop production index CPI_U during 2000–2005 in the Furukawa and Nanjing paddy areas, including best and worst harvest year cases.

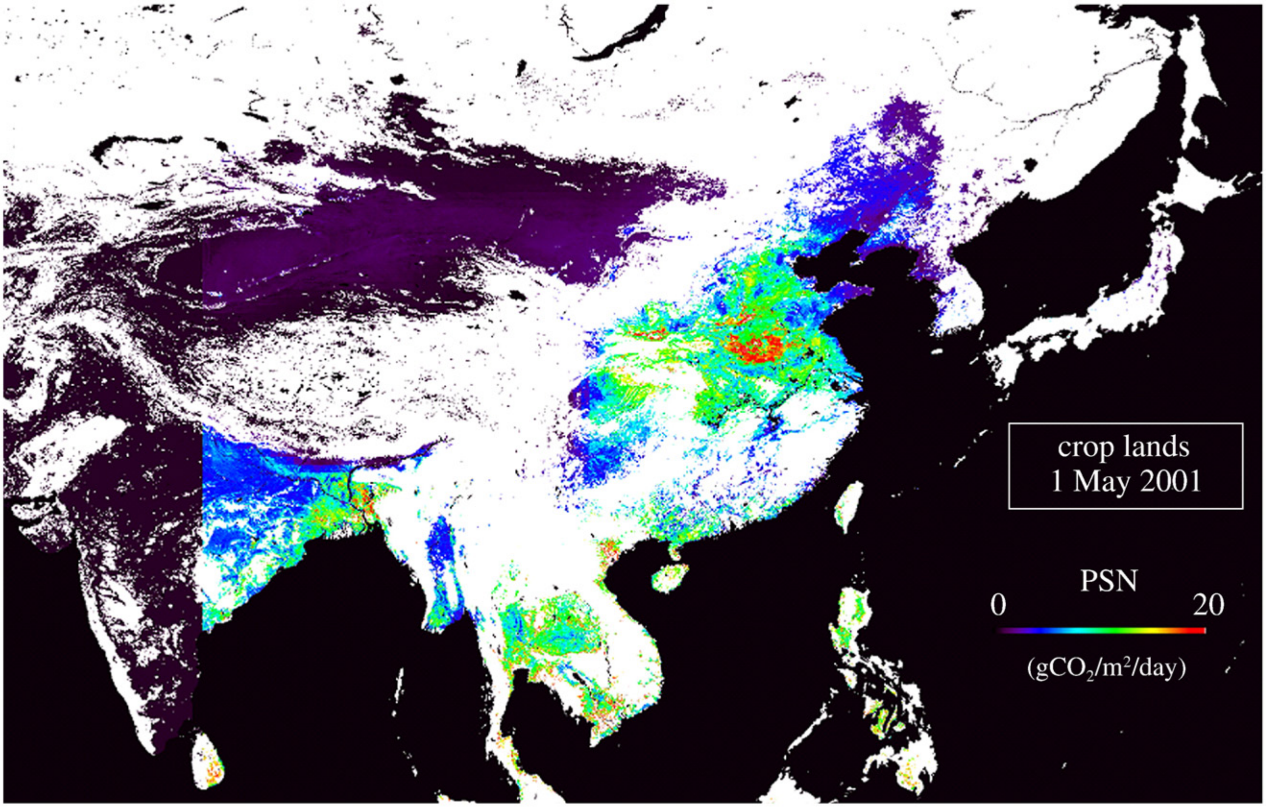

Fig. 7. Distribution of PSN (CO_2 fixation) in grain fields in Southeast Asia on 1 August 2001. The shaded areas in the left side represent the solar radiation coverage derived from Japanese GMS. A decision-tree method using NDVI and LSWI phenology divided the MODIS crop field into four classes: paddy, winter wheat, maize, and other. The PSN is computed using $f_{rad\ pc}$ for paddy, and f_{rad_mm} for winter wheat and maize.

comparison of the former value of carbon in harvested weight of the field yield data with that included in the computations.

5. Discussion

The applicability of the present model depends on whether it is to be used for rice, winter wheat or maize. Results of the comparison for the rice case show good agreement with ground measured harvested data. The differences between carbon contents in grain and carbon fixation estimated by the model are −3.7%, +15.7%, and +15.8%, respectively, in Iwamizawa, Ohogata, and Furukawa in Japan. The estimation error of −1.4% is small and sufficiently accurate for rice monitoring at Nanjing, China. However, the comparison errors are considerably large in the cases of winter wheat and maize. Precisely described, the results of Ohogata in Akita prefecture of northwestern Japan imply that the present model slightly overestimates the photosynthesis rate, resulting in large carbon fixation in good weather conditions. The model slightly overestimates the effects of sterility on the PSN, resulting in a low degree of carbon fixation in bad meteorological conditions. The radiation response function or the constant PSN_{max} of rice can improve the estimation accuracy of the present model in the case of good meteorological conditions. The parameterization of the low-temperature sterility constant k_{Lster} and the Prioul–Chartier constant a_{pc} of Table 3 will also correct these errors. In severe meteorological cases of a bad harvest in 2003, the evaluated errors will be improved by considering the sterility effects in determining the carbon fixation ratio for paddy rice with utilization of the CSI. The last values listed in Table 3 present the final evaluated

Table 1
Weights of carbon included in harvested grains for validation of the photosynthesis model.

Nation	Japan			China			Variable and formulae
Province	Hokkaido	Akita	Miyagi	Jiangsu	Hebei	Shandong	Province
Region	Iwamizawa	Ohogata	Furukawa	Nanjing	Shijiazhuang	Jinan	Region
Grain	Paddy	Paddy	Paddy	Paddy	w_wheat	Maize	Grain
Harvest Index	0.42	0.486	0.507	0.529	0.41	0.46	HI
Year	2001	2001	2001	2001	2001	2001	
Model type	PC	PC	PC	PC	MM	MM	Michaelis–Menten (MM), Prioul–Chartier (PC)
Grain areas (ha) $\times 10^3$ (ha)	24.3	9.33	45.6	2010	2580	2505	A_{grain}
Grain Production $\times 10^3$ (t)	120.0	54.30	247.2	16933	11227	15324	P_{grain}
Yield (t/ha)	**4.94**	**5.82**	**5.42**	**8.42**	**4.35**	**6.12**	$\mathbf{Y_T}$
Dry_W_y (t/ha)	3.55	4.18	3.89	6.05	3.12	4.39	$Y_{DW} = Y_t^* 0.718$
Ratio C/carbohydrate	0.444	0.444	0.444	0.444	0.444	0.444	$R_{CCh} = 72/162$
Carbon_y (tC/ha)	**1.58**	**1.86**	**1.73**	**2.69**	**1.39**	**1.95**	$Y_C = Y_{DW}^* R_{CCh}$
Carbon_fixation_Grain (Production) $\times 10^3$ (t)	38.3	17.3	78.9	5403	3583	4890	$C_{FGP} = Y_{DW}^* R_{CCh}^* A_{grain}$

Table 2
Fixed carbon computed using the photosynthesis model in the grain portion of the plants.

Validation regions		Nation	Japan			China			Variable and formulae
		Province	Hokkaido	Akita	Miyagi	Jiangsu	Hebei	Shandong	Province
		Region	Iwamizawa	Ohogata	Furukawa	Nanjing	Shijiazhuang	Jinan	Region
Conditions		Grain	Paddy	Paddy	Paddy	Paddy	w_wheat	Maize	Grain
		Harvest Index	0.42	0.486	0.507	0.529	0.41	0.46	HI
		Year	2001	2001	2001	2001	2001	2001	
		Model type	PC	PC	PC	PC	MM	MM	Michaelis–Menten (MM), Prioul–Chartier (PC)
Evaluation from this model	CO_2	CO_2 fixation (Model) (gCO_2/m^2)	**2986**	**3654**	**3264**	**4256**	**1592**	**2942**	F_M
		CO_2 fixation (βs) (gCO_2/m^2)	–	–	–	–	1303	2314	$FM\beta$
		CO_2 fixation (tCO_2/ha)	**29.86**	**36.54**	**32.64**	**42.56**	**13.03**	**23.14**	$F_{M\beta t}$
		Respiration_night (tCO_2/ha)	12.33	15.09	13.48	17.58	1.86	9.55	Paddy: $R_N = F_{M\beta t} * 0.413$ Wheat: $R_N = F_{M\beta t} * 0.143$
		Carbon respiration_night (tC/ha)	3.37	4.12	3.68	4.80	0.51	2.61	R_{Nt}
		Net fixation (tCO_2/ha)	**17.53**	**21.45**	**19.16**	**24.98**	**11.16**	**13.58**	$F_{net} = F_{MM\beta t} - R_N$
		Net provincial CO_2 fixation (Million t)	0.43	0.20	0.87	50.2	28.8	34.0	$F_{NPC} = F_{Mt} * A_{grain}/10^6$
	Carbon	Ratio C/CO_2	0.273	0.273	0.273	0.273	0.273	0.273	$R_{CCo} = 12/44$
		Net C fixation (tC/ha)	**4.78**	**5.85**	**5.22**	**6.81**	**3.04**	**3.70**	$C_{FMt} = F_{net} * R_{CCo}$
		C_fixation_aboveGround (tC/ha)	3.61	4.42	3.95	5.15	2.30	2.80	$C_{MFaG} = C_{FMt} * 0.756$
		C_fixation_Grain-only (tC/ha)	**1.52**	**2.15**	**2.00**	**2.72**	**0.94**	**1.29**	$C_{MGt} = C_{MFaG} * HI$
		Provincial C fixation_Grain_Model $\times 10^3$ (t)	36.9	20.1	91.3	5477	2434	3226	$C_{MGA} = C_{MGt} * A_{grain}$
		Provincial C_fixation in whole grain plant $\times 10^3$ (t)	116.2	54.6	238.2	13695	7854	9278	$C_{MNA} = C_{FMt} * A_{grain}$
Ratios and errors		Carbon fixation ratio in Grain (model/yield_data)	0.96	1.16	1.16	1.01	0.68	0.66	$R_{CGF} = C_{MGt}/Y_C$
		Estimation error (%)	**−3.7%**	**15.7%**	**15.8%**	**−1.4%**	**−32.1%**	**−34.0%**	$(1 - R_{CGF}) * 100$

errors. The revised errors are small. They are −3.7% for Iwamizawa in Hokkaido in northern Japan on the side of good harvest in 2001, and 1.4% at Furukawa in Miyagi prefecture of northeastern Japan on the side of a bad harvest in 2003.

Regarding the data for winter wheat and maize, the estimation errors are considerably high because of insufficient sites and crop statistical data in Japan and China used in modeling. For these grains, more validation sites are necessary, but only very few exist in Japan and there are no sufficient crop statistical data to support modeling. The sources of errors are considered as follows.

1) NDVI is sometimes influenced by the cloud effects; therefore, the model tends to underestimate PSN.
2) Yield values vary considerably according to the region, despite almost identical weather conditions. Other factors such as soils and fertilizers also affect the regional yield values.
3) The average yield modeled by the 1 km^2 grid resolution differs from that of 500 km^2 resolution. The mean NDVI in the same area is useful for validation through comparison with carbon partitioning in grain plants in actual fields.
4) The Harvest Index varies widely depending on cultivars, soil fertility and early harvesting for good taste. These factors influence carbon partitioning in grain plants.
5) Regarding the influences by mixels, main interests are in paddy fields, which are covered by water. Almost no other crop can be found in pixels. Winter wheat fields are also easily decomposed from other crops because of the season of harvest in late spring. However, maize, spring wheat and soybean fields are mixed by annual rotation of planting, which is one of the error sources of PSN in the maize fields.
6) Regarding winter wheat and maize, the estimation errors are considerably large because of the dearth of reliable sites and crop statistical data in Japan and China for modeling. The authors intend to apply the present model to other monitoring sites in Australia for winter wheat and maize sites in central U.S.A. to adjust model parameters to fit the yield data.

Table 3
Correction of carbon estimation errors to evaluate sterility effects on carbon fixation ratio for paddy rice using CSI.

Prefecture	Hokkaido		Akita		Miyagi		Variable and formulae
County	Iwamizawa		Ohogata		Furukawa		Province
Year	2001	2003	2001	2003	2001	2003	Year
Harvest situation	Good harvest	Bad harvest	Good harvest	Bad harvest	Good harvest	Bad harvest	Harvest situation
Yield (t/ha)	**4.94**	3.89	**5.82**	5.37	**5.42**	3.65	
Net fixation (tCO_2/ha)	**17.53**	15.14	**21.45**	15.20	**19.16**	15.29	C_{FMt}
C_fixation_Grain-only (tC/ha)	**1.52**	1.31	**2.15**	1.52	**2.00**	1.60	Y_T
Carbon_y (tC/ha)	**1.58**	1.24	**1.86**	1.71	**1.73**	1.16	Y_C
CSI	**101**	**79**	**102**	**94**	**103**	**69**	CSI
Carbon fixation ratio in Grain (model/yield_data)	**0.96**	**1.06**	**1.16**	**0.890**	**1.16**	**1.37**	$R_{CGF} = C_{MGt}/Y_C$
Sterility correction factor subtracted by photosynthesis effect	–	0.84	–	0.99	–	0.74	$f_{ster} = (CSI + CSI100 * 0.05)/CSI100$
Carbon fixation ratio in grain corrected by sterility	No sterility	**0.837**	No sterility	**0.890**	No sterility	**0.945**	RCGF*CSI/100
	No sterility	**0.890**	No sterility	**0.881**	No sterility	**1.014**	$R_{CGF} * f_{ster}$
Estimation error (%)	−3.7%	−16.3%	15.7%	−11.0%	15.8%	−5.5%	E_{CSI}
	−3.7%	**−11.0%**	**15.7%**	**−11.9%**	**15.8%**	**1.4%**	$E_{SterSYN}$

7) The calculation and definition of yield, whether it is by dried weight and grains only, and whether the corncobs are included for the case of maize, can be different. Carbon partitioning methods for model validation require the use of broad test sites with exact and reliable grain statistical data as the case of paddy rice sites in Japan.
8) Fluxnet data will be useful for validation of this model. However, the observed tower data include CO_2 absorption and emission from soil carbon storage. The flux observation must include soil flux to extract CO_2 fixed by the photosynthesis phenomena from ecosystem data using vertical flux distribution data.

The MODIS photosynthesis data are also valuable for comparison with this model but they are not proper for validation because the MODIS data are not observed. They are instead estimated using a light-use efficiency model (Running et al., 1999). On the other hand, tower flux data include an approximately 20% underestimated imbalance (Wilson et al., 2002) in closure of the surface energy balance because of the time variation in low frequency by "bursting" phenomena in eddy structures and because of other energy terms of storage (Meyers and Hollinger, 2004) or respiration at night (Wilson et al., 2002). The authors believe that carbon partitioning is the better means to validate the crop photosynthesis mode.

Concerning the mean net CO_2 and carbon fixation rates in paddy areas for carbon circulation and global warming, those values were, respectively, 19.38 (t CO_2/ha) and 5.28 (t C/ha) in Japan. These values are canopy photosynthesis rates, which include no soil emission and storage, in contrast to the cases of surface-flux ecosystem observation in paddy fields. Meanwhile, the carbon enrichment chamber experiment by Sakai et al. (2001) in Japan provides the maximum gross photosynthesis rate 49.01 (gCO_2/m^2/day), the maximum net photosynthesis rate 36.53 (gCO_2/m^2/day), and the maximum night-time respiration 7.64 (gCO_2/m^2/day) for ambient normal CO_2 concentration, respectively, as control experiments to the elevated CO_2 concentration chambers. The present model slightly overestimates the canopy daytime PSN_{max} in Fig. 3 (Japan) and Fig. 6 (China) on upper-side cases of good meteorological conditions in paddy areas in Fig. 3, and total seasonal carbon fixation values in Fig. 6. Precisely, the daytime mean PSN_{max} of the averaged seasonal variation of PSN that is simulated in Fig. 3 is almost identical to the maximum uptake rate of 39 (gCO_2/m^2/day) of a daily net ecosystem CO_2 exchange observed by Saito et al. (2005) at the Tsukuba FLUXNET station in central Japan. The reason is that the soil flux is around 2.0 (gCO_2/m^2/day) in a flooded paddy, as reported by Yoshida et al. (1974). However, the present model shows the daytime canopy PSN_{max} near 50 (gCO_2/m^2/day) in Fig. 3 on the upper-side cases of good meteorological conditions in paddy areas. The reduction of the maximum nighttime respiration 7.64 (gCO_2/m^2/day) from this daytime PSN_{max} 50 (gCO_2/m^2/day) gives the daily maximum canopy PSN_{max} as 42.4 (gCO_2/m^2/day), which is slightly higher than the maximum net photosynthesis rate of 36.53 (gCO_2/m^2/day) and the maximum daily net ecosystem uptake rate of 39 (gCO_2/m^2/day) including soil flux about 2.0 (gCO_2/m^2/day). This trend is considered to be the same in cases of mean total values of seasonal carbon fixation 19.38 (t CO_2/ha) and 5.28 (t C/ha) in Japan, as described above in this section.

6. Conclusions

In this study, a monitoring system for estimating CO_2 fixation and grain yields is developed by using a photosynthetic sterility model integrating the effects of solar radiation and air temperature on photosynthesis, along with the grain filling from heading to ripening. This modeling system in conjunction with satellite remote sensing data, enables the evaluation of carbon fixation by vegetation on a continental scale and grain yields monitoring in Asia as an operational procedure. An analytical photosynthesis and sterility model is described, which incorporates data related to solar radiation, air temperature and NDVI by assimilating operational meteorological data and satellite data on a global scale. The system is also applicable to important social fields related to global warming such as monitoring desertification and Clean Development Mechanism (CDM) for reduction of CO_2 emission in developing countries. The partitioning of sequestered CO_2 into grain, straw, and root portions of plant biomass weight is computed; the present photosynthesis model is evaluated using the mass of carbon included in the harvested grains of provincial crop production. The applicability of the present modeling system depends on whether it is intended for use with rice, winter wheat or maize. In general, the proposed model yields good results for the case of rice, but it tends to overestimate the photosynthesis rate slightly in good meteorological conditions and underestimate PSN in bad weather conditions by overestimating the sterility effects on rice yields. The parameterization of radiation response function and the temperature response functions for low-temperature sterility can improve the model for the operational monitoring system.

Regarding winter wheat and maize, the estimation errors are considerably large because of the dearth of reliable sites and crop statistical data in Japan and China for modeling. The authors intend to apply the present model to other monitoring sites in Australia for winter wheat and maize sites in central U.S.A. to adjust model parameters to fit the yield data. Regarding the mean CO_2 and carbon fixation rates in paddy areas, those values were, respectively, 25.92 (t CO_2/ha) and 5.28 (t/ha) in Japan, as found in this study.

Acknowledgments

This study is funded by a Grant-in-Aid (no. 21580319) for Scientific Research. We wish to express thanks to the Japan Society for the Promotion of Science, of the Ministry of Education, Culture, Sports, Science and Technology.

References

Aase, J.K., Siddoway, F.H., 1981. Spring wheat yield estimates from spectral reflectance measurements. IEEE Transactions on Geoscience and Remote Sensing GE-19 (2), 78–84.
Cavero, J., Farre, I., Debaeke, P., Faci, J.M., 2000. Simulation of maize yield under water stress with the EPIC phase and CROPWAT Models. Agronomy Journal 92, 679–690.
Cui, J., Kusutani, A., Toyota, M., Asanuma, K., 2000. Studies on the varietal difference of Harvest Index in rice—relationship between harvest index and dry matter production. Japanese Journal of Crop Science 69 (3), 351–358 (in Japanese with English abstract).
Dente, L., Satalino, G., Mattia, F., Rinaldi, M., 2008. Assimilation of leaf area index derived from ASAR and MERIS data into CERES-Wheat model to map wheat yield. Remote Sensing of Environment 112, 1395–1407.
Doraiswamy, P., Sinclair, T., Hollinger, S., Akhmedov, B., Stern, A., Prueger, J., 2005. Application of MODIS derived parameters for regional crop yield assessment. Remote Sensing of Environment 97, 192–202.
Doraiswamy, P.C., Hatfield, J.L., Jackson, T.J., Akhmedov, B., Prueger, J., Stern, A., 2004. Crop condition and yield simulations using Landsat and MODIS. Remote Sensing of Environment 92, 548–559.
Economic Research Institute for ASEAN and East Asia (ERIA), 2008. Symposium on "Energy and Food Strategy for Sustainable Economic Growth in East Asia" in December 2008, Tokyo. http://www.eria.org/seminars/efs.html.
Fang, H., Liang, S., Hoogenboom, G., Teasdale, J., Cavigelli, M., 2008. Corn-yield estimation through assimilation of remotely sensed data into the CSM–CERES–Maize model. International Journal of Remote Sensing 29 (10), 3011–3032.
FAO, Food Outlook-Global Market Analysis – (Rice, Wheat, Maize): http://www.fao.org/docrep/012/ak341e/ak341e05.htm.
FAO FAOSTAT, 2007. Trade—Major Commodity Exporters. http://faostat.fao.org/site/342/default.aspx.
Gao, Y., Jin, G., Chen, H., 1998. Simulating the optimal growing season of rice in the Yangtze River Valley and its adjacent area, China. Agricultural and Forest Meteorology 91, 251–262.
GEO GEOSS, GEOSS themes: Agriculture. http://www.earthobservations.org/geoss_ag.shtml.
Gonzalez, A.D., Chen, P., Lopez, M.T., Srinivasan, R., 2002. Using satellite and field data with crop growth modeling to monitor and estimate corn yields in Mexico. Crop Science 42, 1943–1949.

Hayes, M.J., Decker, W.L., 1996. Using NOAA AVHRR data to estimate maize production in the United States Corn Belt. International Journal of Remote Sensing 17 (16), 3189–3200.
Idso, S.B., Jackson, R.D., Reginato, R.J., 1977. Remote-sensing of crop yields. Science 196, 19–25.
IPCC 5th assessment report, 2009. Food production systems and food security in Impacts, Adaptation, and Vulnerability: http://www.ipcc.ch/pdf/ar5/wg2-outline.pdf.
Jones, J.W., Hoogenboom, G., Porter, C.H., Boot, K.J., Batchelor, W.D., Hunt, L.A., Wilkens, P.W., Singh, U., Gijsman, A.J., Ritchie, J.T., 2003. The DSSAT cropping system model. European Journal of Agronomy 18, 235–265.
Kaneko, D., 2006a. Developing a photosynthetic prediction model for rice yield using remotely sensed and meteorological data. 2nd Recent Advances in Quantitative Remote Sensing. University of Valencia, Valencia, Spain, pp. 549–554.
Kaneko, D., 2006b. Evaluation of CO_2 fixation in Japanese paddy fields by a photosynthesis model using satellite data. Annual Journal of Hydraulic Engineering, Japan Society of Civil Engineers 50, 475–480 (in Japanese with English abstract).
Kaneko, D., 2006c. Estimation of rice situation index in Japan using remotely sensed and meteorological data. Journal of the Remote Sensing Society of Japan 26 (3), 202–212 (in Japanese with English abstract).
Kaneko, D., 2007. Crop yield monitoring based on a photosynthetic sterility model using NDVI and daily meteorological data. The International Society for Optical Engineering, Proceedings of SPIE, Remote Sensing for Agriculture, Ecosystems, and Hydrology IX, 14th SPIE EUROPE International Symposium on Remote Sensing, 6742, F67420. SPIE-The International Society for Optics and Photonics, Firenze, Italy, pp. 1–12.
Kaneko, D., Ohnishi, M., Ishiyama, T., 2003. Proposal of early monitoring method for crop production in China and India In the recent era of water resources restriction. Environmental Systems Research, Japan Society of Civil Engineers 31, 235–244 (in Japanese with English abstract).
Kaneko, D., Ohnishi, M., Ishiyama, T., Tateishi, R., 2004a. Modeling of a photosynthetic crop production index for early warning using NDVI and Meteorological data. International Society for Optical Engineering, Proceedings of SPIE, Remote Sensing for Agriculture, Ecosystems, and Hydrology, 11th SPIE International Symposium on Remote Sensing, SPIE-The International Society for Optical Engineering, Gran Canarias, pp. 1–10.
Kaneko, D., Ohnishi, M., Ishiyama, T., Tateishi, R., 2004b. Proposal of a photosynthesis type of crop yield index for monitoring crop production in China and India in the era of water resource restriction. 4th International Crop Science Congress, 4p, Brisbane, Australia. http://www.cropscience.org.au/icsc2004/poster/2/8/252_dai-jir.htm#TopOfPage.
Kaneko, D., Ohnishi, M., Ishiyama, T., 2005. Photosynthetic rice production index for early warning using remote sensing and meteorological data. SPIE, Remote Sensing for Agriculture, Ecosystems, and Hydrology, 12th SPIE EUROPE International Symposium on Remote Sensing, SPIE-The International Society for Optical Engineering, Bruges, Belgium, pp. 1–9.
Kaneko, D., Kumakura, T., Yang, P., 2008a. Crop yield and CO_2 fixation monitoring in Asia using a photosynthetic-sterility model with satellites and meteorological data. Proceedings of the Global Conference on Global Warming-2008 (GCGW-08), 6–10 July, Istanbul, Turkey, Paper No. 378, pp. 227–238.
Kaneko, D., Kumakura, T., Yang, P., 2008b. Monitoring of crop yields and CO_2 fixation by a photosynthetic-sterility model using satellites and meteorological data in Asia. 5th International Crop Science Congress, Jeju, Korea CS3-S3, No.04. 4pp.
Kaneko, D., Yang, P., Kumakura, T., 2009a. Crop yield and CO_2 fixation monitoring over Asia by a photosynthetic-sterility model comparing with MODIS and carbon amounts in grain yields 34th International Symposium on Remote Sensing of Environment. Agricultural Monitoring TS-2-2, the European Commission Joint Research Centre, Stresa, Italy, pp. 1–4.
Kaneko, D., Kumakura, T., Yang, P., 2009b. Data assimilation for crop yield and CO_2 fixation monitoring in Asia by a photosynthetic-sterility model using satellites and meteorological data. International Journal of Global Warming 1 (3), 179–200.
Kato, M., Yokoo, M., Maruyama, S., 2006. Dry-matter partitioning and accumulation of carbon and nitrogen during ripening in a female-sterile line of rice. Plant Production Science 9 (3), 185–190.
Kogan, F., Yang, B., Wei, G., Zhiyuan, P., Xianfeng, J., 2005. Modeling corn production in China using AVHRR-based vegetation health indices. International Journal of Remote Sensing 26 (11), 2325–2336.
Meyers, T., Hollinger, S., 2004. An assessment of storage terms in the surface energy balance of maize and soybean. Agricultural and Forest Meteorology 125, 105–115.
NASA Goddard Space Flight Center (GSFC), 2010. MODIS land-cover: http://modis-land.gsfc.nasa.gov/landcover.htm.
Prioul, J.L., Chartier, P., 1977. Partitioning of transfer and carboxylation components of intracellular resistance to photosynthetic CO_2 fixation: a critical analysis of the methods used. Annals of Botany, pp. 789–800.
Rasmussen, M.S., 1992. Assessment of millet yields and production in northern Burkina Faso using integrated NDVI from the AVHRR. International Journal of Remote Sensing 13 (18), 3431–3442.
Rasmussen, M.S., 1998. Developing simple, operational, consistent NDVI-vegetation models by application of environmental and climatic information: Part II. Crop yield assessment. International Journal of Remote Sensing 19 (1), 119–137.
Roebeling, R.A., Putten, E.V., Genovese, G., Rosema, A., 2004. Application of Meteosat derived meteorological information for crop yield predictions in Europe. International Journal of Remote Sensing 25 (23), 5389–5401.
Running, S., Nemani, R., Glassy, J., Thornton, P., 1999. MODIS daily photosynthesis (PSN) and annual Net Primary Production (NPP) product (MOD17) –Algorithm theoretical basis document, Version 3.0, Numerical Terradynamic Simulation Group (NTSG), The University of Montana, 59 pp. http://150.131.192.209/modis/ATBD/ATBD_MOD17_v21.pdf.
Saito, M., Miyata, A., Nagai, H., Yamada, T., 2005. Seasonal variation of carbon dioxide exchange in rice paddy field in Japan. Agricultural and Forest Meteorology 135, 93–109.
Sakai, H., Yagi, K., Kobayashi, K., Kawashima, S., 2001. Rice carbon balance under elevated CO_2. The New Phytologist 150, 241–249.
Sasaki, H., Hara, T., Ito, S., Miura, S., Hoque, M.M., Lieffering, M., Kim, H.Y., Okada, M., Kobayashi, K., 2005. Seasonal changes in canopy photosynthesis and respiration, and partitioning of photosynthate, in rice (*Oryza sativa* L.I) grown under free-air CO_2 enrichment. Plant & Cell Physiology 46 (10), 1704–1712.
Sinclair, T.R., 1998. Historical changes in Harvest Index and crop nitrogen accumulation. Crop Science 38, 638–643.
Tanno, H., Kinoshita, M., Kiuchi, H., Hirayama, Y., Kiuchi, H., 2001. Estimation of cool-weather tolerance at the flowering stage and its relation with that at the booting stage in rice varieties in the area south of Tohoku district, Japan. Japanese Journal of Crop Science 70 (2), 209–214.
Tateishi, R., 2001. Twenty-year global 4-minute AVHRR NDVI dataset, CEReS, Chiba University, CD-ROM.
Tubiello, F.N., Rosenzweig, C., Goldberg, R.A., Jagtap, S., Jones, J.W., 2002. Effects of climate change on US crop production: simulation results obtained by using two different GCM scenarios. Part 1: wheat, potato, maize, and citrus. Climate Research 20, 259–270.
Vong, N.Q., Murata, Y., 1997. Studies on the physiological characteristics of C3 and C4 crop species. I. The effects of air temperature on the apparent photosynthesis, dark respiration and nutrient absorption of some crops. Japanese Journal of Crop Science 46, 45–52.
Wiegand, C.L., Richardson, A.J., Richardson, A.J., Jackson, R.D., Pinter Jr., P.J., Aase, J.K., Smika, D., Lautenschlager, L.F., McMurtrey, J.E., 1986. Development of agrometeorological crop model inputs from remotely sensed information. IEEE Transactions on Geoscience and Remote Sensing GE-24 (1), 90–98.
Wilson, K., Goldstein, A., Falge, E., Aubinet, M., Baldocchi, D., Berbigier, P., Bernhofer, C., Ceulemans, R., Dolman, H., Field, C., Grelle, A., Ibrom, A., H., Law, B., Kowalski, A., Meyers, T., Moncrieff, J., Monson, R., Oechel, W., Tenhunen, J., Valentini, R., et al., 2002. Energy balance closure at FLUXNET sites. Agricultural and Forest Meteorology 113 (1-4), 223–243.
Xiao, X., Boles, S., Liu, J., Zhuang, D., Frolking, S., Li, C., Salas, W., Moore, B., 2005. Mapping paddy rice agriculture in southern China using multi-temporal MODIS images. Remote Sensing of Environment 95, 480–492.
Xiao, X., Boles, S., Frolking, S., Li, C., Babu, Y., Salas, W., Moore, B., 2006. Mapping paddy rice agriculture in Southeast Asia using multi-temporal MODIS images. Remote Sensing of Environment 100, 95–113.
Yoneyama, T., Fukuda, M., Kouchi, H., 1989. Partitioning of carbon, Phosphorus, potassium, calcium, and magnesium in a semidwarf high-yielding rice variety: comparison with a conventional Japonica variety. Soil Science and Plant Nutrition 35 (1), 43–54.
Yoshida, S., Coronel, V., Parao, F., Reyes, E., 1974. Soil carbon dioxide flux and rice photosynthesis. Soil Science and Plant Nutrition 20 (4), 381–386.